

All-optical regeneration on a silicon chip

Reza Salem,¹ Mark A. Foster,¹ Amy C. Turner,² David F. Geraghty,¹ Michal Lipson,²
and Alexander L. Gaeta¹

¹ School of Applied and Engineering Physics, Cornell University, Ithaca, NY 14853

² School of Electrical and Computer Engineering, Cornell University, Ithaca, NY 14853
reza.salem@cornell.edu, a.gaeta@cornell.edu

Abstract: We demonstrate optical 2R regeneration in an integrated silicon device consisting of an 8-mm-long nanowaveguide followed by a ring-resonator bandpass filter. The regeneration process is based on nonlinear spectral broadening in the waveguide and subsequent spectral filtering through the ring resonator. We measure the nonlinear power transfer function for the device and find an operating peak power of 6 W. Measurements indicate that the output pulse width is determined only by the bandwidth of the bandpass filter. Numerical modeling of the nonlinear process including free-carrier effects shows that this device can be used for all-optical regeneration at telecommunication data rates.

©2007 Optical Society of America

OCIS codes: (190.4390) Nonlinear optics, integrated optics; (060.4510) Optical communications; (230.1150) All-optical devices; (230.7370) Waveguides; (190.3270) Kerr effect.

References and links

1. P. V. Mamyshev, "All-optical data regeneration based on self-phase modulation effect," in Proc. European Conference on Optical Communications (ECOC'98), p. 475, 1998.
2. J. Yu and P. Jeppesen, "Simultaneous all-optical demultiplexing and regeneration based on self-phase and cross-phase modulation in a dispersion shifted fiber," *J. Lightwave Technol.* **19**, 941–949 (2001).
3. V. G. Ta'eed, M. Shokooh-Saremi, L. Fu, D. J. Moss, M. Rochette, I. C. M. Littler, B. J. Eggleton, Y. Ruan, and B. Luther-Davies, "Integrated all-optical pulse regenerator in chalcogenide waveguides," *Opt. Lett.* **30**, 2900–2902 (2005).
4. A. Bogoni, P. Ghelfi, M. Scaffardi, and L. Poti, "All-optical regeneration and demultiplexing for 160-Gb/s transmission systems using a NOLM-based three-stage scheme," *J. Quantum Electron.* **10**, 192–196 (2004).
5. S. Yamashita, and M. Shahed, "Optical 2R regeneration using cascaded fiber four-wave mixing with suppressed spectral spread," *IEEE Photon. Technol. Lett.* **18**, 1064–1066 (2006).
6. H. Simos, A. Bogris, and D. Syvridis, "Investigation of a 2R all-optical regenerator based on four-wave mixing in a semiconductor optical amplifier," *J. Lightwave Technol.* **22**, 595–604 (2004).
7. M Rochette, L. Fu, V. Ta'eed, D. J. Moss, and B. J. Eggleton, "2R optical regeneration: an all-optical solution for BER improvement," *IEEE J. Sel. Top. Quantum Electron.* **12**, 736–744 (2006).
8. N. Yoshikane, I. Morita, T. Tsuritani, A. Agata, N. Edagawa, and S. Akiba, "Benefit of SPM-based all-optical reshaper for long-haul DWDM transmission systems," *IEEE J. Sel. Top. Quantum Electron.* **10**, 412–420 (2004).
9. M. A. Foster, K. D. Moll, and A. L. Gaeta, "Optimal waveguide dimensions for nonlinear interactions," *Opt. Express* **12**, 2880–2887 (2004), <http://www.opticsinfobase.org/abstract.cfm?URI=oe-12-13-2880>
10. O. Boyraz, P. Koonath, V. Raghunathan, and B. Jalali, "All optical switching and continuum generation in silicon waveguides," *Opt. Express* **12** (17), 4094–4102 (2004), <http://www.opticsexpress.org/abstract.cfm?uri=OE-12-17-4094>
11. E. Dulkeith, Y. A. Vlasov, X. Chen, N. C. Panoiu, and R. M. Osgood., "Self-phase-modulation in submicron silicon-on-insulator photonic wires," *Opt. Express* **14**, 5524–5534 (2006), <http://www.opticsexpress.org/abstract.cfm?uri=OE-14-12-5524>
12. I-W. Hsieh, X. Chen, J. I. Dadap, N. C. Panoiu, R. M. Osgood, S. J. McNab, and Y. A. Vlasov, "Ultrafast-pulse self-phase modulation and third-order dispersion in Si photonic-wire waveguides," *Opt. Express* **14**, 12380–12387 (2006), <http://www.opticsexpress.org/abstract.cfm?id=119784>
13. A. R. Cowan, G. W. Rieger, and J. F. Young, "Nonlinear transmission of 1.5 μm pulses through single-mode silicon-on-insulator waveguide structures," *Opt. Express* **12**, 1611–1621 (2004), <http://www.opticsexpress.org/abstract.cfm?uri=OE-12-8-1611>

14. R. Dekker, A. Driessen, T. Wahlbrink, C. Moormann, J. Niehusmann, and M. Forst, "Ultrafast Kerr-induced all-optical wavelength conversion in silicon waveguides using 1.55 μm femtosecond pulses," *Opt. Express* **14**, 8336–8346 (2006), <http://www.opticsexpress.org/abstract.cfm?uri=OE-14-18-8336>
15. M. A. Foster, A. C. Turner, J. E. Sharping, B. S. Schmidt, M. Lipson, and A. L. Gaeta, "Broad-band optical parametric gain on a silicon photonic chip," *Nature* **441**, 960–962 (2006).
16. Y.-H. Kuo, H. Rong, V. Sih, S. Xu, M. Paniccia, and O. Cohen, "Demonstration of wavelength conversion at 40 Gb/s data rate in silicon waveguides," *Opt. Express* **24**, 11721–11726 (2006), <http://www.opticsexpress.org/abstract.cfm?uri=OE-14-24-11721>
17. Kevin K. Tsia, Sasan Fathpour, and Bahram Jalali, "Energy harvesting in silicon wavelength converters," *Opt. Express* **14**, 12327–12333 (2006), <http://www.opticsexpress.org/abstract.cfm?uri=OE-14-25-12327>
18. Q. Lin, J. Zhang, P. M. Fauchet, and G. P. Agrawal, "Ultrabroadband parametric generation and wavelength conversion in silicon waveguides," *Opt. Express* **14**, 4786–4799 (2006), <http://www.opticsexpress.org/abstract.cfm?uri=OE-14-11-4786>
19. V. R. Almeida, C. A. Barrios, R. R. Panepucci, and M. Lipson, "All-optical control of light on a silicon chip," *Nature* **431**, 1081–1084 (2004).
20. V. R. Almeida, R. R. Panepucci, and M. Lipson, "Nanotaper for compact mode conversion," *Opt. Lett.* **28**, 1302–1304 (2003).
21. L. B. Fu, M. Rochette, V. G. Ta'eed, D. J. Moss, and B. J. Eggleton, "Investigation of self-phase modulation based optical regeneration in single mode As_2Se_3 chalcogenide glass fiber," *Opt. Express* **13**, 7637–7644 (2005), <http://www.opticsexpress.org/abstract.cfm?id=85498>
22. M. R. E. Lamont, M. Rochette, D. J. Moss, and B. J. Eggleton, "Two-Photon Absorption Effects on Self-Phase Modulation-Based 2R Optical Regeneration," *IEEE Photon Technol. Lett.* **18**, 1185–1187 (2006).
23. A. C. Turner, C. Manolatu, B. S. Schmidt, M. Lipson, M. A. Foster, J. E. Sharping, and A. L. Gaeta, "Tailored anomalous group-velocity dispersion in silicon channel waveguides," *Opt. Express* **14**, 4357–4362 (2006), <http://www.opticsexpress.org/abstract.cfm?uri=OE-14-10-4357>
24. C. A. Barrios and M. Lipson, "Modeling and analysis of high-speed electro-optic modulation in high confinement silicon waveguides using metal-oxide-semiconductor configuration," *J. Appl. Phys.* **96**, 6008–6015 (2004).
25. S. F. Preble, Q. Xu, B. S. Schmidt, and M. Lipson, "Ultrafast all-optical modulation on a silicon chip," *Opt. Lett.* **30**, 2891–2893 (2005).
26. A. G. Striegler and B. Schmauss, "Analysis and optimization of SPM-Based 2R regeneration at 40 Gb/s," *J. Lightwave Technol.* **24**, 2835–2833 (2006).
27. T. N. Nguyen, M. Gay, L. Bramerie, T. Chartier, J.-C. Simon, and M. Joindot, "Noise reduction in 2R-regeneration technique utilizing self-phase modulation and filtering," *Opt. Express* **14**, 1737–1747 (2006), <http://www.opticsexpress.org/abstract.cfm?id=88314>

1. Introduction

Impairments caused by dispersion, amplifier noise, and fiber nonlinearities impose limitations on the rate of data transmission in optical communication systems. These deleterious effects can be overcome using optical regeneration techniques that can reshape and "clean-up" the optical signal. As data rates increase, it becomes desirable to perform optical regeneration without relying on high-speed electronic components. Several nonlinear optical techniques have been demonstrated for all-optical signal regeneration, including self-phase modulation (SPM) in fibers or integrated waveguides [1-3], cross-phase modulation [4], and four-wave mixing (FWM) [5-6]. One technique proposed by Mamyshev [1] operates via nonlinear SPM-induced spectral broadening followed by spectral filtering at an offset wavelength. This method is especially attractive not only because it is simple and does not require a second optical signal, but also because it is the only technique known that improves the BER of the signal in addition to reshaping it [7,8]. While most previously demonstrated optical regeneration methods are not integrated into a compact platform, recent work demonstrated an integrated device in chalcogenide waveguide based on the SPM method [3], which requires relatively high peak-power levels of 50 W.

In this work, we demonstrate regeneration based on the SPM method using an integrated silicon device. Silicon is of special interest for integrated photonic devices due to its well-established processing methods and its compatibility with electronic circuits. In addition, the nonlinear index coefficient of silicon is approximately 200 times higher than silica, and the large core-cladding index contrast allows for far tighter optical confinement [9] than can be

achieved in optical fibers. This combination leads to an effective nonlinearity that is approximately 2×10^5 times larger than standard silica fiber. Using this large Kerr-effect, SPM [10-13], cross-phase modulation spectral shift [14], parametric amplification [15], and FWM wavelength conversion [16-18] have been demonstrated. We demonstrate optical regeneration at reasonable power levels using cm-long nanowaveguides. Due to the large effective nonlinearity, the power level required for this device can be readily attained using standard telecom amplifiers.

2. Device design

Figure 1(a) shows the diagram of the silicon-on-insulator (SOI) waveguide device. Self-phase modulation spectral broadening occurs in the waveguide, which is 8-mm long with cross-sectional dimensions of $250 \text{ nm} \times 450 \text{ nm}$. A spectral component at an offset wavelength is isolated in the drop port of a $20\text{-}\mu\text{m}$ -radius ring resonator at the end of the waveguide. The fabrication and design of the waveguide and ring resonator are described in detail in Ref. 19. The linear propagation loss in the waveguide is 3 dB/cm . Based on the effective mode area and the range of values reported for the nonlinear index coefficient n_2 in the literature [15], we estimate the effective nonlinearity γ to be between 150 and $300 \text{ W}^{-1}\text{m}^{-1}$. The transmission of the drop and pass ports of the filter are measured using amplified spontaneous emission as a broadband source, and the measured response is plotted in Fig. 1(b). The free spectral range of the ring resonator is 9 nm , and the bandwidth is 0.75 nm . The center wavelength and the bandwidth of the ring resonator bandpass filter are different for TE and TM polarizations. In addition, the waveguide dispersion and loss depend on the light polarization. The device can operate for a fixed TE- or TM-polarized input signal. We carefully adjust the input light polarization to be TM for all of our measurements including the filter spectral response shown in Fig. 1(b).

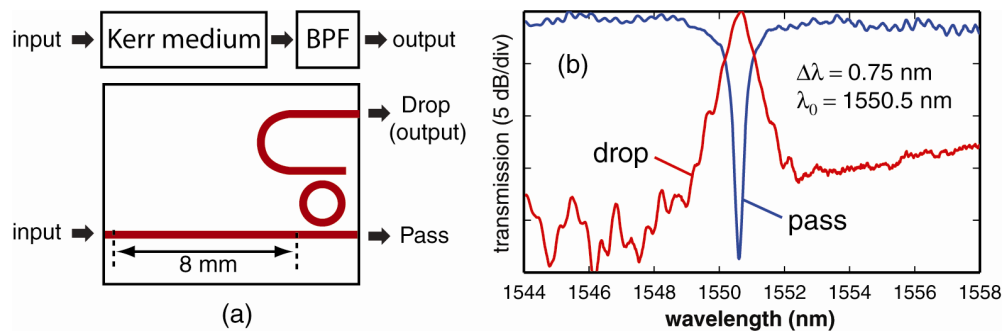


Fig. 1. (a) Diagram of the regenerator device. BPF: band-pass filter. (b) Measured transmission spectra of pass and drop ports of the ring resonator for TM polarization.

3. Experiment

Figure 2(a) depicts the experimental setup used to measure the nonlinear power transfer function of the device. Optical pulses are generated from a femtosecond optical parametric oscillator centered at 1550 nm with 75-MHz repetition rate. A 1-nm bandpass filter centered at 1552 nm is used to produce 3.5 ps pulses. The signal is amplified, TM-polarized and coupled into the waveguide using a tapered lens fiber and an inverse taper mode converter on the silicon chip [20]. The optical pulses are first sent into a waveguide that has the same cross-section and length as the regenerator device but without the ring resonator. This allows us to measure the spectral broadening of the pulses going through the silicon waveguide. Figure 2(b) plots the broadened spectra for different peak pump powers, as estimated inside the waveguide at the input. The plot corresponding to the lowest peak power (0.2 W) in Fig. 2(b) shows the pulse spectrum with no broadening effect. Due to the low duty cycle of the pulses,

SPM in the EDFA is unavoidable and it results in the sidebands seen in the pulse spectrum, even without broadening in the silicon waveguide (green curve in Fig. 2(b)). In order to assure that the SPM process in the EDFA does not cause any regeneration effect, we have varied the signal power going into the silicon waveguide using an attenuator after the EDFA while the EDFA power is kept constant. As the input power is increased, the pulse spectrum undergoes up to 3 nm of broadening as a result of SPM. At high peak powers, a blue-shift due to the phase shift induced by the generated free carriers [10,11] results in an asymmetry in the broadened spectrum. As shown in Fig. 1(b), the center wavelength of the ring bandpass filter is 1550.5 nm, which is 1.5 nm away from the center wavelength of the input pulse. Even without broadening, a small fraction of the power passes through the filter, since it has an extinction ratio of only 15 dB at the center of the input spectrum. As the peak power of the input signal increases, the spectrum broadens and more power is coupled into the drop port of the ring resonator. Figure 2(c) plots the spectra measured at the of the drop port of the ring for different pulse peak powers.

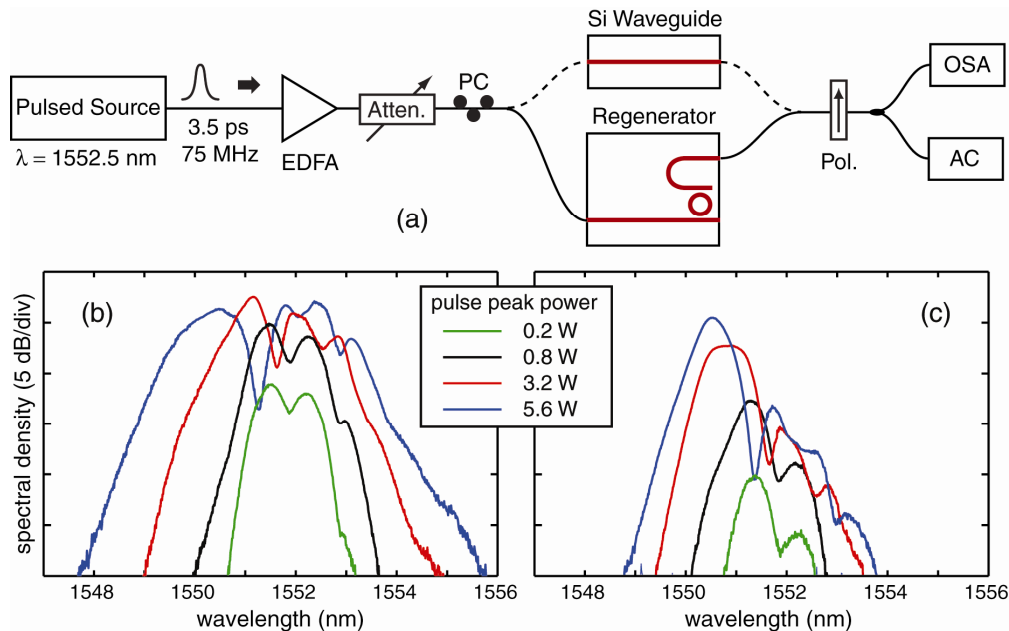


Fig. 2. (a) Experimental setup used for measuring the power transfer function of the regenerator. The waveguide without ring resonator is used to measure the broadened spectrum. (b) Broadened spectra for different pulse peak powers after passing through the silicon waveguide without the ring resonator. (c) Output spectra from the drop port of the ring resonator (regenerator output).

4. Power transfer function and autocorrelation measurements

To characterize the nonlinear power transfer function for our device, the input power is varied using an optical attenuator, while the output power is measured by integrating the output spectrum as shown in Fig. 2(c). The measured power transfer function for the device is plotted in Fig. 3(a). In an ideal regenerator, a flat response is desired at high power levels. However, the SPM-broadened spectrum is not completely flat, and the power transfer function exhibits ripples at high power levels. It has been shown that normal group-velocity dispersion (GVD) and two-photon absorption (TPA) in the nonlinear medium reduce these ripples [21,22]. Silicon exhibits a significant amount of TPA at 1.5 μm , making it a suitable material in this regard. In addition, we designed the waveguide to have a high normal GVD, which we estimate to be about $-15000 \text{ ps/nm}\cdot\text{km}$. The dispersion is estimated using a finite-difference

mode solver described in our earlier work [23]. An ideal regenerator based on SPM is expected to have a quadratic power transfer function at low powers. Inspection of Fig. 3(a) shows that the response is between linear and quadratic, which is caused by poor extinction ratio of the ring filter. Figure 1(b) indicates that the filter extinction ratio at the signal wavelength is less than 15 dB, and this low extinction ratio is also evident from Fig. 2(c).

The transfer function is simulated using numerical modeling of the pulse propagating in the silicon waveguide. A range of values are reported in the literature for nonlinear index and TPA coefficients, and we choose values that are in the range of reported values and that provide the best fit of the experimental data to the numerical model. The values used in the numerical model are $n_2 = 7.5 \times 10^{-14} \text{ cm}^2/\text{W}$ for nonlinear index coefficient and $\beta = 0.8 \text{ cm/GW}$ for the TPA coefficient, and the free-carrier lifetime for the device is taken to be 450 ps [19]. The effect of free carriers generated by TPA on both the refractive index and the loss of the waveguide [10,24] is considered. It is important to note that the carrier lifetime is much shorter than the time between the pulses, and thus the free carriers generated by each pulse recombine before the second pulse arrives. The dashed curve in Fig. 3(a) shows the simulation result for our device. The ring-resonator response used in the simulation matches our measurements shown in Fig. 1(b). In order to show how the power transfer function can be improved at low powers, we show simulation results with a Gaussian filter and with two cascaded ring resonators. The filters have the same bandwidth as the single ring resonator, and the results are shown in Fig. 3(b) for the three different filters. It can be seen that by using two cascaded ring resonators, the transfer function is improved and differs only slightly from that of the Gaussian filter.

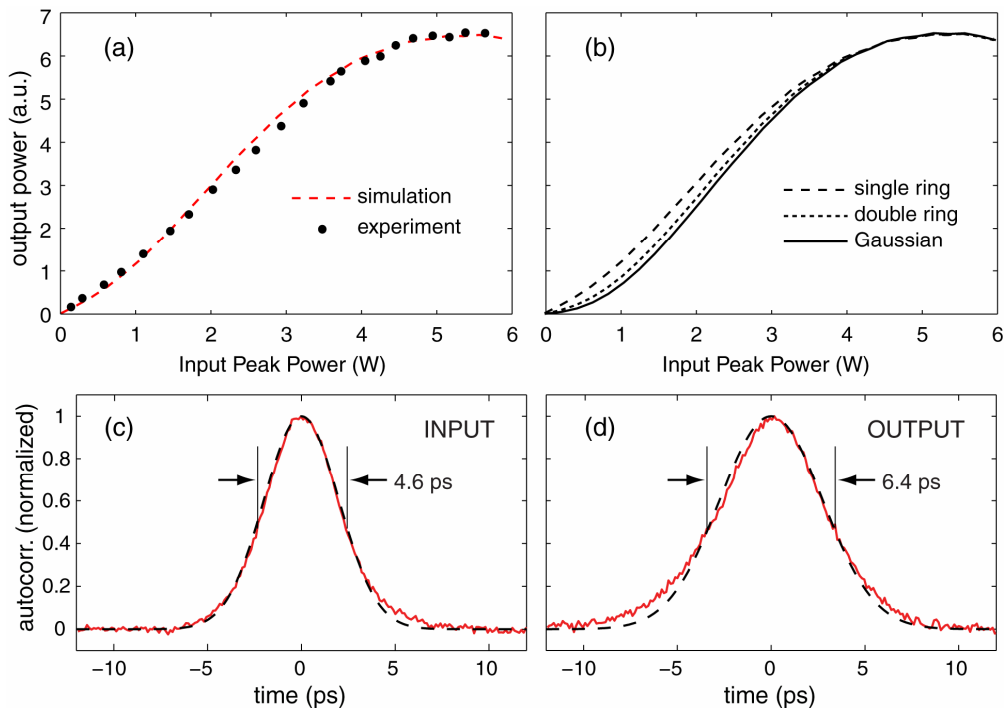


Fig. 3. (a) Measured power transfer function for the device and numerical simulation (dashed curve). (b) Numerical simulation of the power transfer function for different output filters. (c) Input pulse autocorrelation and that of a Gaussian profile with the same FWHM (dashed line). (d) Output autocorrelation and that of a Gaussian profile with the same FWHM.

In order to characterize the duration of the input and output pulses, we measure their autocorrelation. Figure 3(c) plots the autocorrelation measurement for the input pulse, and the

dashed curve represents a Gaussian function with the same FWHM as the measured autocorrelation, which is 4.6 ps. Assuming a Gaussian pulse shape for the input, the FWHM of the input pulse is 3.3 ps. The dispersion length for these pulses inside the silicon waveguide is about 25 cm, which is much longer than the length of the waveguide, and suggests that there should be minimal dispersive broadening. Due to the coupling efficiency and the sensitivity of the autocorrelator, the output power from the regenerator is not high enough to perform a direct autocorrelation measurement. In order to measure the output, the pulses are amplified and filtered with a 1-nm bandpass filter for ASE noise removal. Figure 3(d) shows plots of the autocorrelation measurement for the output pulse and the Gaussian profile matching the FWHM of the measured autocorrelation, which is 6.4 ps. It can be seen that the output autocorrelation differs from the Gaussian function possibly due to the addition of a 1-nm bandpass filter at the output or to the non-Gaussian response of the ring filter. If we approximate the output pulse with a Gaussian function, the FWHM of the pulse is 4.5 ps. The pulse broadening (3.3 ps to 4.5 ps) is mainly attributed to the ring filter at the output of the regenerator having a narrower bandwidth than the input pulse spectral width. The EDFA used for the autocorrelation measurement has a negligible dispersive effect on the output pulse. We estimate that the 1-nm bandpass filter used before the autocorrelator leads to a 10% temporal broadening. Another effect of this filter is to remove the part of the spectrum that is not completely rejected due to the poor extinction ratio of the ring resonator. In our simulations these spectral components are dominant at low power levels, but their effect is very small at high powers at which the autocorrelation measurements were performed. In order to preserve the initial pulse shape, the ring resonator should be designed to have a bandwidth matching the input spectral width.

5. Discussion

The free-carrier lifetime of the device used in these experiments is 450 ps. As mentioned earlier, the blue-shift caused by the modulation of free-carrier density contributes to the final output of the regenerator. The blue shift results from the rapid change in the free-carrier density as the pulse enters the waveguide. If residual free carriers are present from a previous data pulse, then the blue shift is reduced. Therefore, at data rates higher than 1 Gb/s, some data pattern dependence is expected. However, it has been shown that by using a pn junction that sweeps the carriers out of the device, the free-carrier lifetime can be significantly decreased. Based on the currently reported research, the carrier lifetime can be as low as 30 ps [25], allowing for data rates beyond 10 Gb/s. In order to model the performance of this device at these higher data rates, we consider a similar device but with a free-carrier lifetime equal to 30 ps. Random data with 3.5 ps pulse width at 10 Gb/s rate is considered as the input to this device and the simulation is performed for 1000 random bits. The 6-W peak power required for device operation demands an average power of 100 mW, which is readily available from standard amplifiers. As seen in Fig. 3(b), cascaded ring resonators can generate a power transfer function that is very close to the transfer function of the device with a Gaussian filter. Therefore, for simplicity, we have assumed a Gaussian filter for the following simulations.

5.A Suppression of amplitude jitter and ghost pulses

The amplitude of the logical 1's in a digital data signal can fluctuate due to various causes. This amplitude jitter can be reduced using the SPM-based 2R regenerator [26]. The suppression of amplitude jitter is caused by the flat power transfer function at high power levels as shown in Fig. 3(a). Similarly, another impairment in digital communication systems is caused by having low power pulses, called ghost pulses, instead of logical 0's. These low-power pulses are caused by nonlinearities in fiber and can be suppressed by the SPM-based 2R regenerator as well [26]. A simple way to model amplitude jitter and ghost pulses is to vary the power at the logical 1's and 0's randomly by a certain percentage. The mean peak power of the 1's is adjusted to achieve optimal regeneration, and the maximum amplitude variations of the 1's and 0's are set to 15% and 10% of this optimal value respectively. Figure 4(a) shows plots of the eye diagram of the data at the input and output of the regenerator

showing the suppression of both ghost pulses and amplitude jitter. In order to make a better comparison between the two eye diagrams, the time scale is marked based on the FWHM pulse width of either the input or the output pulses. The small asymmetry seen in the output eye diagram is due to the data pattern dependence caused by the free-carrier effect.

5.B Noise reduction and BER improvement

Another way to evaluate the performance of the device is to consider a data signal mixed with random noise. This type of numerical analysis has been done for SPM-based regenerators that use fiber as the nonlinear medium [7,27]. In our model, random noise is generated with a flat amplitude spectrum and a random phase. The noise is added to the RZ data signal with perfect extinction ratio and is passed through a bandpass filter. It has been shown that the frequency response of this input filter can affect the regeneration performance significantly [27]. We use a fifth-order super-Gaussian response with 2-nm bandwidth, which provides the maximum improvement of the quality factor. The optical signal-to-noise ratio (OSNR) is defined as the average power of the signal divided by the power in 0.1 nm bandwidth of the noise. Figure 4(b) shows plots of the eye diagram for the input and output data signal with OSNR = 14 dB. It has been shown previously [27] that the SPM-based regenerator cannot completely eliminate the random noise due to the phase-amplitude coupling in the nonlinear process. We estimate the Q -factor with and without regeneration, and the values are shown in Fig. 4(c) indicating a 3-dB improvement in the Q -factor. The estimation of the Q -factor is done by calculating the standard deviation of the peak power of the logical 1's. The effect of noise is much more significant on the logical 1's than on the 0's. Therefore, if the peak power associated with the logical 1's has a mean value of μ_1 and standard deviation of σ_1 , we can estimate the Q -factor to be $Q \approx \mu_1/\sigma_1$.

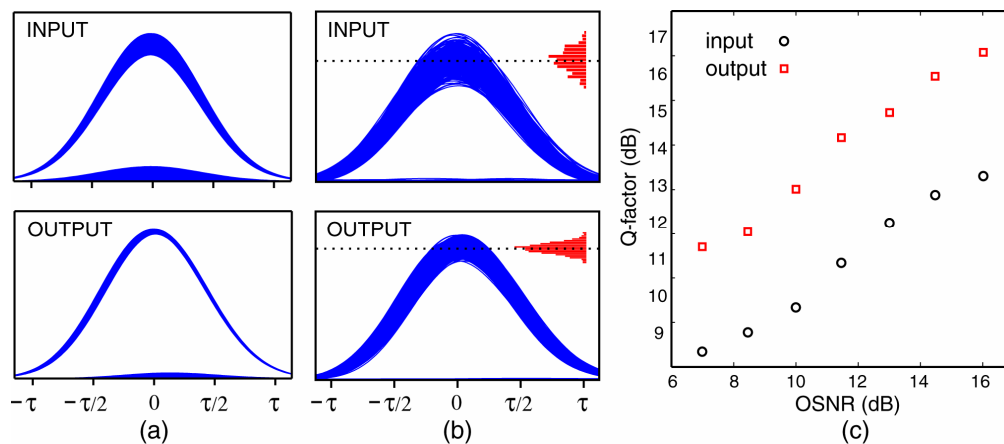


Fig. 4. (a) Simulated eye diagrams of the data at the input and output of the regenerator when amplitude and ghost pulses are present. (b) Simulated eye diagrams of the noisy data at the input and output of the regenerator (histogram for the peak power of the logical 1's is shown). (c) Estimated Q -factor of the input and output for the case of noisy input.

6. Conclusion

We have demonstrated an integrated, silicon-based optical regenerator based on spectral broadening in a nanowaveguide followed by a ring resonator. The nonlinear power transfer function of the device is measured, and the operating peak power is found to be less than 6 W. Autocorrelation measurements of the input and output pulses show that the output pulse width is mainly determined by the ring resonator bandwidth. Improvement in the power transfer function is expected by fabricating output filters with a higher extinction ratio. Free-carrier effects contribute to the nonlinear spectral broadening in the waveguide through the

modulation of refractive index, and this effect is expected to cause data pattern dependence if the free-carrier lifetime is longer than the bit period. We numerically analyzed the performance of the regenerator device for 10-Gb/s RZ signal assuming a free-carrier lifetime equal to 30 ps, which has been achieved in silicon nanowaveguide devices. Reduction of amplitude jitter, ghost pulses and random noise was shown by the numerical simulations and we expect that higher data rates can be achieved by using devices with even shorter carrier lifetimes.

Acknowledgments

We acknowledge financial support from the DARPA DSO Slow-Light Program and the Center for Nanoscale Systems, supported by the NSF and the New York State Office of Science, Technology & Academic Research. M.A.F. acknowledges support via the IBM Graduate Fellowship Program.